

A Re-radiation Model for the Earth's Energy Budget and the Albedo Advantage in Global Warming Mitigation

Alec Feinberg, DfRSoft Research, email: dfrsoft@gmail.com

Abstract

A solar geoengineering re-radiation model is developed for the global mean Earth's energy budget (GMEEB) and results provide new insights. The GMEEB is depicted in terms of re-radiation events. We apply the model to 1950 and 2019 to illustrate its capability. To obtain the GMEEB, modeling only requires solar energy input, the re-radiation factor, and the amount of greenhouse gas (GHG) forcing. The model then predicts the GMEEB with and without forcing. A 61.8% optimum re-radiation factor is found in modeling in the absence of forcing. Above or below this value, iterative transition states occur. We demonstrate the possible transitional states and how they may converge to a new GMEEB with its re-radiation GHG change. Results suggest that albedo controls have many advantages in reducing global warming. We find about 38% less reverse forcing would be needed for global albedo increases compared to GHG reductions to mitigate climate change.

Key Words: Re-Radiation Model, Earth's Energy Budget, Albedo Advantage, Albedo-GHG Factor, Solar Geoengineering, reverse forcing

1. Introduction

Re-radiation modeling is important for global warming solar geoengineering solutions [1] and provides an alternate way to view the Earth's Energy Budget in terms of re-radiation events. The model is helpful in geoengineering estimates and provides insights into albedo mitigation advantages discussed in Section 4. An optimum re-radiation parameter (in the absence of forcing) is found to have a unique value of 0.618 (or β^4). This parameter can be taken as a redefined variable of the effective emissivity constant for the planetary system. Given either the Earth's surface temperature or the global albedo value, the GMEEB in the unforced thermal equilibrium re-radiation steady state can be determined. Certainly, other re-radiation values can occur as the atmosphere is dynamic. However, we define this as the baseline GMEEB re-radiation state. We apply this condition to 1950, treating this as a pseudo time in which no forcing occurs and reasonable results are found. This assumption allows us to make approximations for application insight. Figure 1 illustrates our result that provides a view of the global mean Earth's energy budget in what we term the repeatable re-radiation baseline steady-state (without forcing).

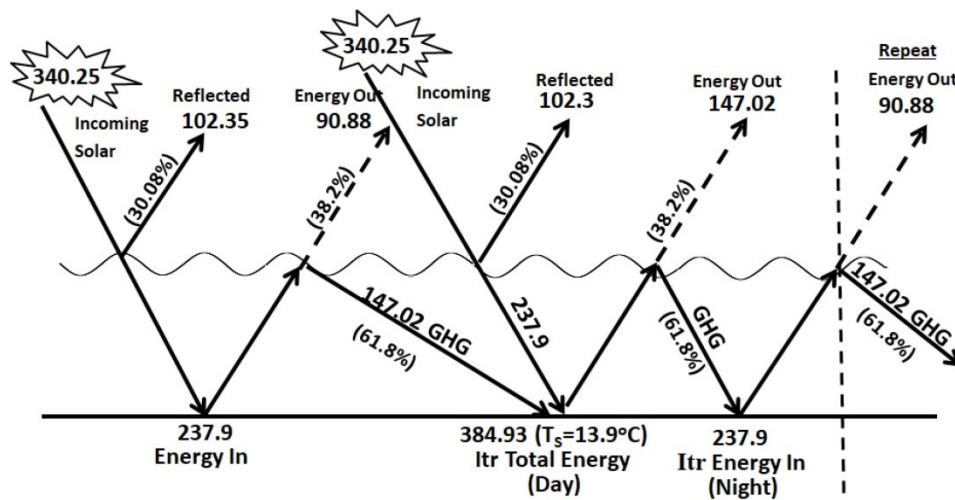


Figure 1 1950 Baseline stable time series iterative re-radiation GMEEB (values in W/m^2)

The figure illustrates how the sequential time series iterative re-radiation events are repeatable. When the atmosphere fluctuates in GHG content, the transition states can differ from the GMEEB baseline shown in Figure 1. However, this is viewed as the yearly average. Using a similar diagram, we show how the states could transition to obtain the 2019 GMEEB re-radiation state as an example. The wave line in Figure 1 is used to conceptualize the mean interactions between the atmosphere and radiation events. Note that the warming energy imparted to the surface is obtained simply as the addition of the solar input and mean GHG re-radiation yielding the global mean 1950 value of $384.93 \text{ Watts}/m^2$ (13.9°C). The ‘Iterative (Itr) Energy In,’ is exactly equal to the initial ‘Energy In’ and the ‘Iterative Total Energy’ is also repeatable when the GHG re-radiation value is 61.8%. Also, no imbalance is observed between the energy in and out.

The re-radiation estimate for 1950 is comparable to the value of Kiehl et al. 1997 [2]. They determined a total longwave GHG re-radiation of $155 \text{ W}/m^2$ and a clear sky re-radiation of $125 \text{ W}/m^2$. Given that cloud coverage is roughly 67%, the weighted average is $145 \text{ W}/m^2$ in 1990. This is very close to the $147 \text{ W}/m^2$ estimate in Figure 1 due to the optimum 61.8% re-radiation condition derived in our model and illustrated in Figure 1. From the figure, the average absorbed albedo ‘Energy In’ is multiplied by 1.618 re-radiation factor to obtain the $384.93 \text{ W}/m^2$.

Applications of these models are provided for two different periods (1950 and 2019). In 2019 modeling requires a time series transient solution. However, the iterative transitional energy states converge and we identify the convergence as the GMEEB re-radiation steady state for 2019. Since the atmosphere is dynamic, it can be helpful to view some of the iterative transition states. As the atmosphere is in flux, transitional states and their convergent condition can be found for the available GHG forcing content although the goal is to represent GMEEB steady state for 2019.

2. Data and Method

The planetary budget concept is often written

$$C \frac{dT_S}{dt} = F_{TOA} \quad (1)$$

with C the Earth's heat capacity and F_{TOA} , the top-of-the-atmosphere (TOA) radiative flux so that

$$F_{TOA} = \frac{S_o}{4}(1-\alpha) - \sigma T_e^4 = P_\alpha - \sigma T_e^4 \quad (2)$$

Here T_S is the surface temperature, and $S_o=1361\text{W/m}^2$. When the planet is in equilibrium, $dT_S/dt=0$. At equilibrium

$$P_\alpha = \frac{S_o}{4}(1-\alpha) = \sigma T_e^4 = \sigma T_\alpha^4 = \beta^4 \sigma T_S^4 = \beta^4 P_{Total} \quad (3)$$

The definitions of $T_\alpha=T_e$, and β are the emission temperature, surface temperature, and typically $\beta \approx 0.887$, respectively. Here we use a slightly different notation than commonly used by introducing T_α instead of T_e . Now writing

$$P_{Total} = \frac{P_\alpha}{\beta^4} = \sigma T_S^4 = \frac{\sigma T_\alpha^4}{\beta^4} \quad (4)$$

When initial solar absorption occurs, part of the long-wavelength radiation given off is re-radiated back to Earth as depicted in Figure 1. In the absence of forcing, we denote this average re-radiation fraction \bar{f}_1 . At this point, we present a simplistic but effective re-radiation model (as illustrated in Fig. 1)

$$P_{Total} = P_\alpha + P_{GHG} = P_\alpha + \bar{f}_1 P_\alpha = P_\alpha (1 + \bar{f}_1) = \sigma T_S^4 \quad (5)$$

Referring to Figure 1, P_α is the 'Energy In', P_{GHG} is the GHG re-radiation energy, P_{Total} is the "Total Energy'. Here \bar{f}_1 turns out to be exactly β^4 in the absence of forcing, so that \bar{f}_1 is a redefined variable taken from the effective emissivity constant of the planetary system. We identify $1+\bar{f}_1=1.618034$ (in Section 2.1) as the global average 'albedo-GHG' radiation factor (Table 1) since it yields the sum effect from re-radiation and solar input.

2.1 The Baseline Steady State Re-radiation Solution

We are considering a time when there are *no forcing issues* causing warming trends. Then by conservation of energy, the equivalent power re-radiated from GHGs in this model is dependent on P_α with

$$P_{GHG} = P_{Total} - P_\alpha = \sigma T_S^4 - \sigma T_\alpha^4 \quad (6)$$

To be consistent typically $T_\alpha \approx 255^\circ\text{K}$ and $T_S \approx 287^\circ\text{K}$, (see Table 3 results) then in keeping with a common definition of the global beta (the proportionality between surface temperature and emission temperature) we have $\beta \approx T_\alpha/T_S = T_e/T_S$.

This allows us to write the dependence

$$P_{GHG} = \sigma T_S^4 - \sigma T_\alpha^4 = \frac{\sigma T_\alpha^4}{\beta^4} - \sigma T_\alpha^4 = \sigma T_\alpha^4 \left(\frac{1}{\beta^4} - 1 \right) = \sigma T_\alpha^4 \left(\frac{1}{\bar{f}} - 1 \right) \quad (7)$$

Note that if $\beta^4=1$, there would be no GHG effect. Here we set \bar{f} , the re-radiation parameter equal to β^4 .

We can also define the re-radiation similarly by some fraction f_1 such that

$$P_{GHG} = \bar{f}_1 P_\alpha = \bar{f}_1 \sigma T_\alpha^4 \quad (8)$$

According to Equations 7 and 8, we require

$$P_{GHG} = \sigma T_\alpha^4 \left(\frac{1}{\bar{f}} - 1 \right) = \bar{f}_1 \sigma T_\alpha^4 = \bar{f} \sigma T_\alpha^4 \quad (9)$$

When $\bar{f} = \bar{f}_1$ the solution is derived from the quadratic expression

$$\bar{f}^2 + \bar{f} - 1 = 0 \text{ yielding } \bar{f} = 0.618034 = \beta^4, \beta = (0.618034)^{1/4} = 0.88664 \quad (10)$$

This is very close to the common value estimated for β and it was obtained through energy balance in the planetary system providing a non-series exact solution per Eq. 10. This is the unique stable baseline re-radiation state illustrated in Figure 1. Although the atmosphere is dynamic and other non-forcing alternate states can exist, we use this value for the optimum repeatable baseline steady-state GMEEB re-radiation solution. This steady-state solution may be the lowest thermodynamic re-radiation free energy condition (see next section). In solar geoengineering, we can view the re-radiation as part of the albedo effect. Consistency with the Planck parameter is shown in Appendix A. We note the assumption $\bar{f} = \bar{f}_1$ only works if planetary energy is in balance without forcing. In Appendix B, Eq. 10 is derived in another way by balancing energy in and out of our global system showing full agreement with this result.

2.2 Thermodynamic stable re-radiation baseline state

Although not the point of this paper, we suggest that the baseline state ($\bar{f} = 0.618$) is likely the lowest thermodynamic re-radiation free energy steady state for any global albedo value. We might argue that it is the lowest free energy state because away from this condition, higher energy flow appears to be required to converge (see Sec 2.4).

2.3 Method for Estimating Global Nominal Average Re-radiation Strength for 1950

Global warming can be exemplified by looking at two different periods. The model in Equation 5 can be applied for 1950 which we take as a pseudo baseline period where we assume the following

- no forcing issues causing a warming trend in 1950,
- the average baseline re-radiation value 0.618 is applicable for 1950

then combining Eq. 5 and 10, we are now able to write P_{Total} in terms of the ‘albedo-GHG’ factor

$$P_{Total_1950} = (1 + f_{1950})P_{\alpha} = 1.618P_{\alpha} \tag{11}$$

Here f_{1950} has been set equal to f_1 . This provides a baseline number for our solar geoengineering estimates so that 1.618 becomes the 1950 albedo-GHG reference value. As Figure 1 illustrates, the re-radiation factor (0.618) yields a $P_{\alpha} = 147W/m^2$ value close to the results of that reported by other authors [2]. This reference value is constrained by energy balance in Eq. 9. The actual values in Figure 1 will be exemplified in Section 3 for 1950.

2.4 Time Series Transient States for 2019

Deviations from the nominal 61.8% optimum value due to dynamics in the atmosphere and/or GHG forcing in the industrial era cause transient states and modeling requires series solutions. Figure 2 shows the time series iterative process that we modeled. Time series convergence is found. Figure 2 only shows 2 to 3 iterations. Table 1 provides iteration n=1 through n=10 with the convergent n=10 time series condition.

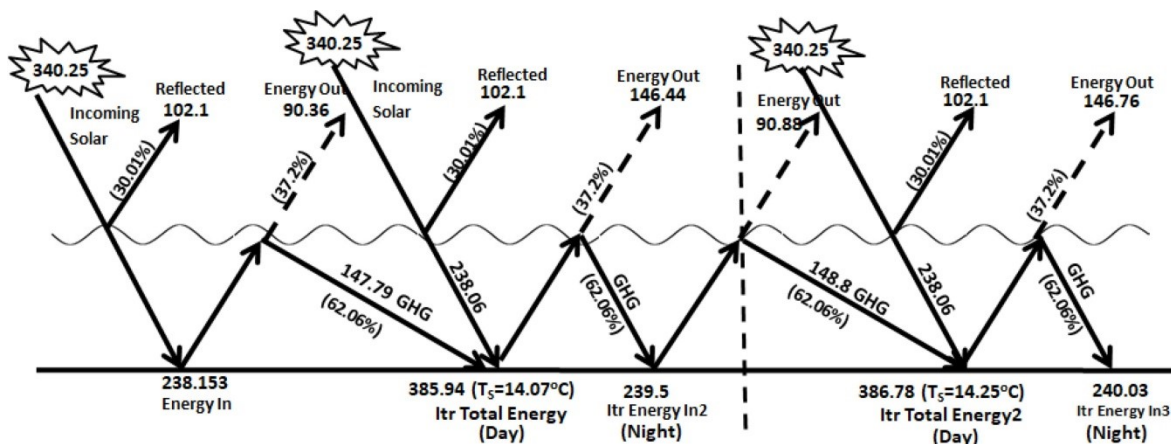


Figure 2 2019 Time series iterative re-radiation events (values in W/m^2)

Unlike feedback, which takes time to be realized due to the Earth's heat capacity, we do not expect as much of an atmospheric lag in GHG forcing. That is, GHG pollution, builds up slowly over time (1950 to 2019). In terms of making estimates, we are interested in quasi-equilibrium conditions for which

transition states occur as in Figure 2 that converge (see Table 1). The goal is the steady-state re-radiation condition for GMEEB. So these are yearly relative re-radiation model average estimates for 1950 and 2019 based on global mean temperature data for these years.

From Table 1, after 10 iterations, re-radiation stability is reached and the energy out (n=10) is equal to the energy in (n=1). At this point, the temperature has stabilized to 0.45°K (n=10) above the 1950 baseline period (see Sec 3) without feedback.

2.5 Method for Iterative Series Convergence in 2019 Transition States

Considering the forcing due to an increase in GHG and a decrease in reflectivity to our climate, it generally happens slowly from 1950 to 2019. The increase in radiative forcing, denoted by R, changes Eq. 1 so that

$$C \frac{dT_s}{dt} = R + F_{TOA} \quad (12)$$

At this point, $dT_s/dt \neq 0$ and transient states occur until a new quasi-equilibrium GMEE condition is reached. Equation 5 can be written in a similar form for the 2019 re-radiation model (initially without feedback) where the primes indicate an increased change

$$P_{Total2019}(t) = P_{\alpha'} + P_{GHG'}(t) = P_{\alpha'}(1 + \bar{f}_{Sum}) \quad (13)$$

To simplify our task, we assume the new global albedo change, $P_{\alpha'}$ does not vary in time. As well we treat \bar{f}_{Sum} as the average 2019 re-radiation value in the final quasi-steady-state GMEE condition.

The GHG-radiative forcing is then (see Table 3)

$$R = P_{Total_2019} - P_{Total_1950} \quad (14)$$

And the energy balance is

$$0 = E_{in}(n=1) - E_{out}(n=N) \quad (15)$$

From Figure 2 and Table 1, we determined the iterative time series solution for any GHG transition n^{th} state as

$$f_{Sum} = f_{2019} = \sum_{n=1}^{N=10} (f^{2n} + f^{2N-1}) = f^2 + f^4 + f^6 + \dots + f^{19} \quad (16)$$

In Appendix C, we provide details on using this sum for obtaining all values in Table 1: $P_{\alpha', n=N}$,

$P_{Total2019_N}$, P_{Out1_N} , P_{Out2_N} with examples for $P_{out1_N=4}$, $P_{out2_N=4}$, Itr Energy In, $P_{\alpha', n}$ for $n=4$, and the surface total $P_{Total_2019_N}$ for $n=4$ notated as $P_{Total2019_4}$.

Table 1 Iterative Time Series Convergence

Quantity Iteration Transitional States	n=1	n=2	n=3	n=4	n=5	n=6	n=7	n=8	n=9	n=10 Stable Maximum State
Itr Energy in (W/m ²) $P_{\alpha'_{n=N}}$	238.15	239.50	240.03	240.23	240.30	240.33	240.34	240.35	240.35	240.35
Itr P _{GHG} $P_{total} - P_{\alpha'}$	147.8	148.6	149.0	149.1	149.1	149.1	149.2	149.2	149.2	149.2
Itr Energy1 out (W/m ²) P_{Out1_N}	90.36	90.88	91.07	91.15	91.18	91.19	91.19	91.20	91.20	91.20
Itr Energy2 out (W/m ²) P_{Out2_N}	146.44	146.76	146.88	146.93	146.94	146.95	146.95	146.96	146.96	146.96
Total Energy Out (W/m ²) (Out_{l+2})	236.80	237.63	237.95	238.08	238.12	238.14	238.15	238.15	238.15	238.15
Surface P Total 2019 (W/m ²) $P_{Total2019_N}$	385.94	386.8	387.1	387.2	387.3	387.30	387.3	387.3	387.3	387.31
Tsurface rise 2019 (°K)	287.2	287.39	287.45	287.47	287.48	287.48	287.49	287.49	287.49	287.49
T rise above 1950 (°K)	0.19	0.35	0.41	0.43	0.44	0.44	0.45	0.45	0.45	0.45

The series must sum to \bar{f}_{Sum} . The estimated average value, analogous to Equation 8, yields the 2019 value given by (see Sec. 3 for applications)

$$f_{2019} = \bar{f}_{Sum} = \bar{f}_{1950} + \Delta\bar{f} = \bar{P}_{GHG_2019} / P_{\alpha_2019} \tag{17}$$

Table 2 shows f and its targeted time series convergence f_{sum} for 1950 and 2019 (Eq. 16). We added f=0.60 as an interesting transitional re-radiation state.

Table 2 $f_{SUM}(f)$ Values of Interest

Key Values	f	f _{Sum}
f < f ₂₀₁₉	0.62057	0.6263
f = f ₁₉₅₀	0.618	0.618
f < f ₂	0.60	0.563

As a check, note that if f is set to the optimal value f=0.618, then the series converges to the same value yielding $f_{sum}=0.618$, as expected, in agreement with the non-series exact solution found in Equation 10. Next, note that if f < 0.618, then $f_{sum} < f$ and if f > 0.618, then $f_{sum} > f$.

2.6 Energy Forcing Transition States and Imbalance

In Table 1, energy forcing is the difference between the total energy as

$$\Delta P_{\text{Forcing}} = (P_{\text{Total}_{n=10}})_{2019} - (P_{\text{Total}})_{1950} = 387.308 \text{ W/m}^2 - 384.927 \text{ W/m}^2 = 2.38 \text{ W/m}^2 \quad (18)$$

This forcing from 1950 to 2019 (extrapolated from IPCC/NOAA estimates, see Sec. 3) is exemplified in Section 3 and Table 3.

The energy imbalance, taken as the difference between $E_{\text{in}_{n=1}}$ and $E_{\text{out}_{n=10}}$, is equal to zero (Table 3).

3.0 Results

The re-radiation model may seem a bit confusing. However, in an application, only Equations 5, 11, 13, and 17 are needed for obtaining the re-radiation GMEEBs. These equations are incredibly simple but very helpful in solar geoengineering. While transitional states are illustrative and more formal, the main focus for presenting them is to support Figures 1 and 2 and the basic idea of re-radiation convergence to the steady equilibrium state condition.

In 1950 we simplify estimates by assuming the re-radiation parameter is fixed and reasonably given by the optimum average value for $f_1=0.618$ yielding a P_α value in reasonable agreement with other authors [2]. Then, to obtain the 1950 average surface temperature, $T_{1950}=13.89^\circ\text{C}$ (287.04°K), the only adjustable parameter left in our model is the global albedo (see also Eq. 5). This requires an albedo value of 0.3008 (see Table 3) to obtain $T_{1950}=287.04^\circ\text{K}$. This albedo number is reasonable and similar to the values cited in the literature [3]. From these values, the 1950 GMEEB diagram in Figure 1 is obtained. Given the incident solar radiation (340.25 W/m^2) and the albedo value, then ‘Energy in’ is $P_\alpha=237.9 \text{ W/m}^2$, and from Eq. 11, $P_{\text{Total}}=384.94 \text{ W/m}^2$, and $P_{\text{GHG}}=384.94 \text{ W/m}^2-237.9 \text{ W/m}^2=147.1 \text{ W/m}^2$ (Eq. 6). These values are summarized in Table 3, row 3.

In 2019, we add a small albedo decline creating 0.25 W/m^2 of forcing that the author has estimated in another study [6] due to surface reflectivity losses related to Urban Heat Islands (UHIs). This also helps provide insight for albedo forcing effects (see Sec. 4.2). Given the incident solar radiation (340.25 W/m^2) and the marginally lower albedo value, then ‘Energy in’ is slightly higher than 1950 at $P_\alpha'=238.15 \text{ W/m}^2$. Next, we use IPCC/NOAA values for GHG forcing as a way to estimate it in our model. We assume most of the forcing is due to GHGs. We adjusted our model to obtain the IPCC/NOAA GHG forcing estimate; we extrapolated from their tables for the period between 1950 and 2019, yielding 2.38 W/m^2 [4, 5]. We then subtracted our albedo forcing of 0.25 W/m^2 to be consistent with total forcing estimates and the author’s prior work [6].

The GHG re-radiation forcing is then part of f_{Sum} in Equation 13 and 16. When f_{Sum} is adjusted to 0.6263 in Eq. 13, then $P_{\text{Total}_{2019}} = 1.6263 \times 238.15 = 387.31 \text{ W/m}^2$ and $P_{\text{GHG}} = 387.31 - 238.15 = 149.15 \text{ W/m}^2$, which

is the GHG value shown in Column 7, and the required forcing value 2.38 W/m^2 [4, 5] relative to 1950 is obtained as required and also matching the same results in Eq. 18. In Table 3, the 2019 row is a summary without feedback. To incorporate feedback, an amplification factor is estimated as $A_F=2.15=0.95 \text{ }^\circ\text{C}/0.45^\circ\text{C}$. Therefore, the feedback is estimated on the known temperature change in 2019. Here we apply feedback as a separate term at the end in the last row in Table 3.

In general, feedbacks estimates values are difficult to quantify [7], but our estimate is consistent with the temperature rise for 2019. The true feedback could eventually be larger due to climate inertia.

Table 3 Model Results

Year	$T_s(^{\circ}\text{K})$	$T_a(^{\circ}\text{K})$	f_{2019} f_{1950}	α, α'	P_α Energy In W/m^2	P_{GHG} P_{GHG}	P_{Total} W/m^2
2019	287.48	254.57	0.6263	30.00065	238.153	149.155	387.308
1950	287.04	254.51	0.6180	30.08	237.903	147.024	384.927
$\Delta 2019-1950$	0.44	0.067	0.0083	(0.244%)	0.25	2.13	2.38
$\Delta_{\text{Feedback}} A_F=2.15$	0.95	0.144	-	-	0.5377	4.58	5.12

In the last row in Table 3, the feedback amplification factor A_F has been incorporated into the forcing model in the following manner

$$P_{\text{Total}2019\&\text{Feedback}} = P_{1950} + (\Delta P) A_F = P_{1950} + (P_{2019} - P_{1950}) A_F = \sigma T_S^4 \tag{19}$$

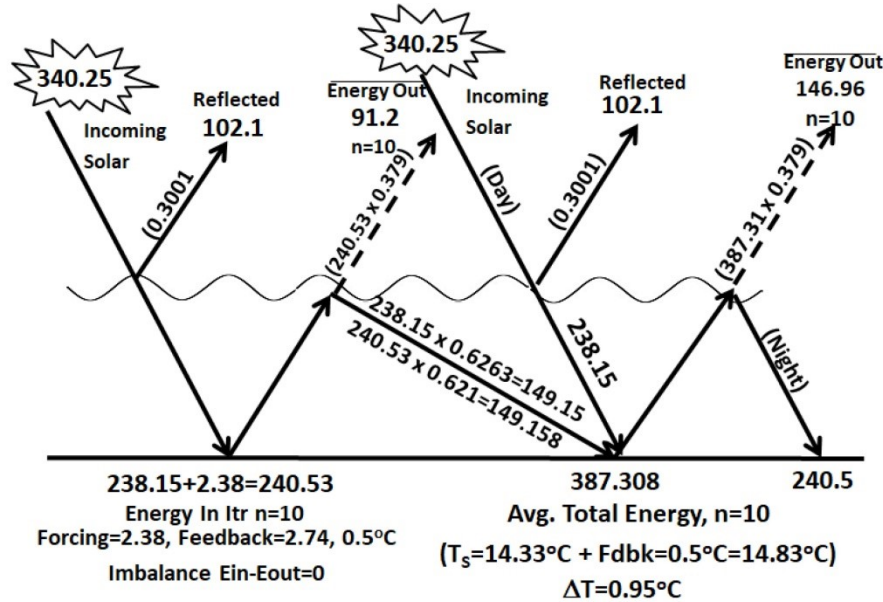


Figure 3 2019 Re-radiation GMEEB with forcing & feedback from Table 3, n=10 (in W/m^2)

We note that the forcing is given by $\Delta P_{\text{GHG}}=2.13 \text{ W/m}^2$ when added to the albedo forcing change yields a total forcing of $\Delta P_{\text{Total}}=2.38 \text{ W/m}^2$. Figure 3 illustrates the 2019 GMEEB for the n=10 transitional state. The re-radiation may be obtained using $f=0.621$ or $f_{\text{sum}}=0.6263$ (see Eq. 16) as indicated in Figure 3. Finally, the imbalance in the diagram, Energy In – Energy Out=0 is relative to the n=1 value of $E_{in}=238.06 \text{ W/m}^2$. As well, unlike f_{1950} , f_{2019} is not a strict measure of the emissivity due to the increase in GHGs (see Appendix A, Eq. A-3).

4.0 Discussion on the Importance of the Albedo Solution to Global Warming

Policymakers should recognize the need for albedo management in global warming mitigation. Here we focus on albedo mitigation strategies because of the lack of attention in this area. Although albedo solutions have been recommended for mitigation of climate change [1, 8-16] and could be a vital complement to CO₂ reduction efforts, little work is being done in this area. There have been several proposed albedo solutions to reduce climate change using both surface and atmospheric strategies [1, 8-16]. These measures have not been widely adopted by governments [15] and were not part of the Paris Climate Accord [17]. In this section, we will discuss several advantages of the albedo solution, based on the findings of this study.

4.1 The Reverse Forcing Albedo Advantage due to the Albedo-GHG Re-radiation Factor

From Table 1 or Figure 1 and 2-3, the 'Energy In' is effectively increased by the average 'albedo-GHG' re-radiation factor of 1.62. For example, in 1950 the surface energy is

$$1.618 \times 287.9 \text{ W} / \text{m}^2 = 384.9 \text{ W} / \text{m}^2 \quad (20)$$

The 1.62 albedo-GHG factor is a combined effect of solar radiation and GHG re-radiation, therefore it is always higher than the GHG re-radiation itself. Thus, as a mitigation strategy, reverse GHG forcing requires the full 2.38 W/m² amount. But because of the albedo-GHG re-radiation compounding effect (with the same albedo for 2019), albedo reverse forcing would only require 1.46 Watts/m², i.e.,

$$1.626 \times 1.46 \text{ W} / \text{m}^2 = 2.38 \text{ W} / \text{m}^2 \quad (21)$$

This is a 38% reverse forcing reduction from 2.38 W/m² to 1.46 W/m². This reverse forcing albedo advantage can be illustrated in Equation 5 and 13 by looking at the rate of change for P_{Total} where

$$\left(\frac{dP_{Total}}{dP_{\alpha}} \right)_{1950} = (1 + f_{1950}) = 1.618 \quad \text{and} \quad \left(\frac{dP_{Total}}{dP_{\alpha}} \right)_{2019} = (1 + f_{2019}) = 1.6263 \quad (22)$$

However, the rate of change due to GHGs is only

$$\frac{dP_{Total}}{dP_{GHG}} = \frac{d(P_{\alpha} + P_{GHG})}{dP_{GHG}} = 1 \quad (23)$$

This helps demonstrate this concept.

A simple way for policymakers to remember and understand this advantage can be illustrated as follows:

- *Increasing the reflectivity of a hotspot surface reduces its greenhouse gas effect*
- *Decreasing the reflectivity of a hotspot surface increases its greenhouse gas effect*

- *The Global Warming change associated with a reflectivity hotspot modification is given by the albedo-GHG radiation factor which has an approximate average value of 1.62, that is, an increase in reflectivity is 62% more effective than a similar reduction in GHG.*

4.2 Percent Albedo Change Required for Reverse Forcing

It is helpful to know what percent global albedo change is required for reverse forcing described in Equation 21 for the $1.46W/m^2$ value. To obtain this estimate, note that from Table 1, a useful value can be described, we denote as the albedo-gamma parameter

$$\gamma_{\% \Delta \alpha} = \frac{(\Delta E_o)_\alpha}{\frac{\alpha_1 - \alpha_2}{\alpha_1} 100} = \frac{0.25W/m^2}{0.244\% \Delta \text{albedo}} = 1.02W/m^2 / \% \Delta \text{albedo} \quad (24)$$

This gamma-albedo value can then be applied to Equation 21 to answer our question. The results for reverse forcing assessment that indicates the required percent global albedo change needed is

$$\text{Reverse Forcing \% Albedo Change} = 1.46W/m^2 / 1W/m^2 / \% \Delta \text{albedo} = 1.46\% \quad (25)$$

For example, for a global albedo of 30.0% in Table 3, the change would be $0.0146 \times 30.00065\% = 0.438$. The global albedo would need to increase from 30.0% to 30.438%.

It is interesting to note that this albedo-gamma parameter in Equation 24 can be derived more formally by considering an albedo change from two different periods. Here a global albedo change from α_1 to α_2 results as follows [1]

$$\gamma_{\% \Delta \alpha} = \frac{S_o / 4 (\alpha_1 - \alpha_2)}{\frac{\alpha_1 - \alpha_2}{\alpha_1} 100} = \frac{S_o}{4} \alpha_1 / 100 \approx 1W/m^2 / \% \Delta \text{albedo} \quad (26)$$

Considering the incoming solar radiation $S_o = 1361W/m^2$ and if $\alpha_1 = 0.3$, the albedo-gamma parameter is approximately $1.02W/m^2 / \% \Delta \text{albedo}$ in agreement with Eq. 24.

4.3 Percent Sunshading Required for Reverse Forcing

Space mirrors on satellites is a concept considered for GW mitigation by changing the amount of solar radiation that falls on the Earth's surface through deflection of sunlight [8, 18, 19]. This shades the Earth. The amount of shading required for reverse forcing of $2.38W/m^2$ estimated in Eq. 18 and Sec. 3, so the required sunshading is

$$\gamma_{\% \Delta P} = \frac{P_{\text{shade}} - P_{2019}}{P_{2019}} = -\frac{\Delta P_{\text{Forcing}}}{P_{2019}} = -\frac{2.38}{387.308} = -0.615\% \quad (27)$$

This is close to the albedo change on the Earth found in Section 4.2 of 0.44%, each having a slightly different estimate related to GHG re-radiation.

4.4 Global Warming Albedo Solution Advantages for Humidity

Mitigating global warming by increasing reflectivity has several advantages in the area of humidity feedback and forcing problems. Many of these advantages could be realized if the reflectivity of Urban Heat Islands (UHIs) could be increased. One important advantage is for UHIs in humid areas. Here we identify three main humidity effects that require albedo management.

1. Zhao et al. [20] observed that UHI temperatures increase in daytime ΔT by 3.0°C in humid climates but decrease ΔT by 1.5°C in dry climates. They found a strong correlation between ΔT increase and daytime precipitation. Their results concluded that albedo management would be a viable means of reducing ΔT on large scales.

This effect is often attributed to greenspace decrease of surface roughness due to UHI impermeable smooth surfaces which reduces convection cooling efficiency (Zhao et al. [20], Gunawardena et al [21]). However, UHIs create high evaporation rates and some degree of convection cooling so perhaps this is not the full reason that explains this effect. Another possible reason we might consider is that since air over cities is warmer and warm air holds more water vapor, this could promote a local GHG effect and be partly responsible for the observed warming. These effects may to a lesser extent occur on all smooth hot evaporating surfaces (during precipitation periods) including roads and highways. Nevertheless, the primary mitigating factor in all these cases would be the albedo management of impermeable surfaces.

2. From the change in the GMEEB, the Earth's temperature has increased since 1950 from 287.04°K to 287.99°K in 2019 (Table 3), which will create more atmospheric water vapor (since warm air holds more water vapor). This is a dominant feedback mechanism contributing to global warming, which some authors estimate doubles the effect of the forcing (Dessler [22], Manabe et al. [23]). The only way to remove water vapor out of the atmosphere and back into the rain budget is through atmospheric cooling. This is a huge undertaking to expect it can fully be accomplished solely by CO_2 reduction, especially in the presence of a high rate of deforestation. Considering the albedo reverse forcing advantage, UHI albedo controls [1, 6] and other reflectivity solutions are urgently needed as a supplement and should be advocated by policymakers. It is important to realize that without UHI albedo controls, urbanization growth can offset albedo reverse forcing efforts, similar to the way deforestation can offset CO_2 reduction efforts making UHI albedo management highly needed.
3. In a study of wetland reduction in China and its correlation to drought, Cao et. al. [24] looked at the wetland distributions and areas for five provinces due to urbanization. These areas showed a total reduction in southwestern China from 1970 to 2008 of 17% ground area, with the highest reduction rate occurring from 2000 to 2008. They found these changes to the wetland area showed a negative correlation with temperature (i.e. wetland decrease, increase in temperature), and a positive correlation with precipitation (i.e. wetland decrease, precipitation decrease). One can conclude that albedo management of urbanization would help increase the loss in

condensation. Although some cities find increases in precipitation due to complex warming turbulence, the larger picture indicates that UHIs are a cause of drought.

4. Drought feedback leads to forest fire feedbacks that not only damage forests that would otherwise remove CO₂ from the air, but that also releases CO₂ and other GHGs into the atmosphere. Therefore, this is a major offset in CO₂ worldwide reduction efforts. This suggests the urgent need for supplementary albedo reverse forcing efforts.

As concluded by Zhou et al. [20], albedo management is an important aspect of UHI global warming humidity mitigation strategies.

4.0 Conclusion

In this paper, we use re-radiation modeling to present an alternate way to view the GMEEB. These results suggest several solar geoengineering assessments and albedo-based climate change mitigation strategies.

We found an optimum pre-industrial global mean re-radiation value of 0.618 which allows for repeatable energy balance (see Fig. 1) without requiring convergent transitional states. We considered this the baseline re-radiation state. The baseline parameter can be taken as a redefined variable of the effective emissivity constant for the planetary system ($\beta^4=0.618$). This allows one to estimate either the Earth's albedo or surface temperature when one of these is known. We applied this factor to 1950, treating this period as a pseudo-pre-industrial year. Results provide a re-radiation GMEEB for 1950 shown in Figure 1. The 'Energy In' is increased by the combined 1.618 'albedo-GHG' factor for 1950 to obtain the total energy.

Outside the optimum re-radiation value required additional time-series transition events for convergence. The convergence solution was obtained in series form. However, the re-radiation model for the GMEEB is easy to use and was applied for the 2019 time period that included forcing and feedback considerations. In the present day, the mean re-radiation factor was found to increase to 0.6276 due to the addition of GHGs.

Because greater attention is being paid to the reduction of CO₂ and other GHGs, we focused on providing insights for albedo solutions. We noted that mitigation of the global warming that occurred from 1950-2019 would require GHG reverse forcing of 2.38 W/m² or alternately a 1.46 W/m² change due to albedo management (a 38% reduction in the magnitude of required mitigation). This resulted from the albedo-GHG 1.626 factor (i.e., 1.626 x 1.46 W/m²=2.38 W/m²). We also identified an albedo-gamma parameter equal to about 1 W/m²/% Δ albedo. The albedo-gamma parameter applied to the 1.46 W/m² value indicates an albedo change of approximately 1.46% global reflectivity increase would be required to mitigate the warming that has occurred since 1950. For a global albedo of 30.000%, the global albedo increase needed would be 30.438% (where 0.0146x30.00065=0.438).

Lastly, we noted that UHI albedo management would have important benefits related to humidity climate change effects. These include reducing the warming humidity effect in cities, drought reduction, and lowering GHG local atmospheric water vapor through cooling.

The following albedo management suggestions and corrective actions are recommended:

- Modification of the Paris Climate Agreement to include albedo controls and solutions
- Albedo guidelines for UHI impermeable surfaces, cool roofs, and roads similar to on-going CO₂ efforts
- UHI albedo goals: we suggest an albedo increase by a factor of 4 (from typical UHI albedo value of 0.12), which could reduce GW by about 30% or more, based a study by the author [6]
- Government funding for geoengineering and implementation of albedo solutions
- Centralize albedo solution efforts in a single government agency (possibly NASA)
- Guidelines for future albedo design considerations of urbanization areas such as requiring all new building to have flat roofs with highly reflective surfaces
- Requires cars to be more reflective. Although world-wide vehicles do not comprise much of the Earth's solar area, recommending the preferential manufacturing of cars that are higher in reflectivity (e.g., silver or white) would raise awareness of this issue similar to electric automobiles that help improve CO₂ emissions.

Appendix A: *Re-radiating Model Consistency with Beta and the Planck Parameter*

It is of interest to show model consistency with beta as it is tied to the re-radiation factor (see Eq.10). Using temperatures obtained from modeling in Table 3 from the two different periods (see Eq. A.3) we note

$$\beta_{1950} = \frac{T_a}{T_s} = \frac{T_e}{T_s} = \frac{254.51}{287.04} = 0.88667 \text{ and } \beta_{1950}^4 = 0.61809 \quad (\text{A.1})$$

And in 2019

$$\beta_{2019} = \frac{T_a}{T_s} = \frac{T_e}{T_s} = \frac{254.57}{287.49} = 0.885 \text{ and } \beta_{2019}^4 = 0.6145 \quad (\text{A.2})$$

These values are reasonably consistent. We also note that

$$f_{2019} = \beta_{2019}^4 + \Delta f \approx f_{1950} + \Delta f = \beta_{1950}^4 + \Delta f = 0.618 + 0.0083 = 0.6263 \quad (\text{A.3})$$

The 0.0096 value is noted in Table 3. This yields the expected re-radiation factor $f_{2019}=0.6276$.

The re-radiation model also is consistent with the Planck parameter. Results in Table 3, show the following estimates for the Planck parameter [25]

$$\lambda_o = -4 \frac{\Delta R_{LWR}}{T_s} = -4 \left(\frac{237.9W/m^2}{287.04^\circ K} \right)_{1950} = -3.315W/m^2/^\circ K \quad (\text{A.4})$$

and

$$\lambda_o = -4 \frac{\Delta R_{LWR}}{T_S} = -4 \left(\frac{238.15 W / m^2}{287.49^\circ K} \right)_{2019} = -3.314 W / m^2 / ^\circ K \quad (A.5)$$

We note these are very close in value showing minor error and consistency with Planck parameter value, often taken as $-3.3 W/m^2/^\circ K$ [25].

Appendix B: Balancing P_{out} and P_{in} in 1950

Although f_1 has been uniquely defined in Eq. 10, this should also result from balancing the energy in and out of the GMEEB. In equilibrium, the radiation that leaves must balance P_α energy in. Then from the GMEEB in Figure 1

$$\begin{aligned} Energy_{Out} &= (1-f_1)P_\alpha + (1-f_1)P_{Total} = (1-f_1)P_\alpha + (1-f_1)\{P_\alpha + f_1P_\alpha\} \\ &= 2P_\alpha - f_1P_\alpha - f_1^2P_\alpha = Energy_{In} = P_\alpha \end{aligned} \quad (B.1)$$

This is consistent, so that in 1950 Eq. B.1 requires the same quadratic solution as Eq. 10. It is also apparent that

$$P_\alpha = \frac{P_{Total_1950}}{1+f_1} = f_1 P_{Total_1950} = \beta_1^4 P_{Total_1950} \quad (B.2)$$

since

$$f_1 = \frac{1}{1+f_1} \quad (B.3)$$

also yields Eq. 10. As a final check, an application in Section 3, Table 3 results, and illustrates that f_1 provides reasonable results.

Appendix C: Table 1 Assessments

The n^{th} energy state is from the time series in Table 1 and applies to Eq. 16 as given by

$$P_{\alpha'_{n=N}} = P_{\alpha'}(f_{sum}/f) = P_{\alpha'}(f + f^3 + f^5 + \dots + f^{2N-2}) = P_{\alpha'} \sum_{n=1}^N (f^{2n-1} + f^{2N-2}) \quad (C.1)$$

Then from Eq. 13, the time series for P_{total} is

$$P_{Total2019_N} = P_{\alpha'}(1 + \bar{f}_{Sum_N}) = P_{\alpha'} \{1 + (f^2 + f^4 + f^6 + \dots + f^{2N-1})\} = P_{\alpha'} \left\{1 + \sum_{n=1}^N (f^{2n} + f^{2N-1})\right\} \quad (C.2)$$

P_{out1} from Figure 2 is $(1-f)$ times the energy in and given as

$$P_{Out1_N} = P_{\alpha'_{n=N}}(1-f) = P_{\alpha'}(1-f) \sum_{n=1}^N (f^{2n-1} + f^{2N-2}) \quad (C.3)$$

Similarly, P_{out2_N} from Figure 2 is $(1-f)$ times the energy in and given as

$$P_{Out2_N} = P_{Total2019_N}(1-f) = P_{\alpha'}(1 + \bar{f}_{Sum_N})(1-f) = (1-f)P_{\alpha'} \sum_{n=1}^N (f^{2n} + f^{2N-1}) \quad (C.4)$$

Example: Itr Energy In, $P_{\alpha'_n}$ for $n=4$

$$\begin{aligned} P_{\alpha'_n=4} &= P_{\alpha'}(f + f^3 + f^5 + f^6) = 238.15W / m^2 (0.6206 + 0.6206^3 + 0.6206^5 + 0.6206^6) \\ &= 240.23W / m^2 \end{aligned} \quad (C.5)$$

Example: Surface Total $P_{Total_2019_N}$ for $n=4$

$$\begin{aligned} P_{Total2019_4} &= P_{\alpha'}(1 + \bar{f}_{Sum_N=4}) = P_{\alpha'} \{1 + (f^2 + f^4 + f^6 + f^7)\} \\ &= 238.15W / m^2 \{1 + 0.6206^2 + 0.6206^4 + 0.6206^6 + 0.6206^7\} = 387.2W / m^2 \end{aligned} \quad (C.6)$$

Example: $P_{out1_N=4}$

$$P_{Out1_N} = P_{\alpha'_n=4}(1-f) = 240.23W / m^2(1-0.6206) = 91.15W / m^2 \quad (C.7)$$

Example: $P_{out2_N=4}$

$$P_{Out2_N} = P_{Total2019_N}(1-f) = 387.2W / m^2(1-0.6206) = 146.93W / m^2 \quad (C.8)$$

Disclosures

Funding: This study was unfunded.

Submission Declaration: This article has not been published previously and is not under consideration elsewhere.

Conflicts of Interest: The author declares that there are no conflicts of interest.

References

1. Feinberg A., On Geoengineering and Implementing an Albedo Solution with UHI GW and Cooling Estimates vixra 2006.0198, DOI: 10.13140/RG.2.2.26006.37444/6 (Currently in Peer Review in the J. Mitigation and Adaptation Strategies for Global Change)
2. Kiehl, J.T. and Trenberth, K.E., 1997: Earth's Annual Global Mean Energy Budget. Bull. American Meteorological Society, Vol.78, 197–208
3. Stephens G., O'Brien D., Webster P, Pilewski P, Kato S, Li J, (2015) The albedo of Earth, *Rev. of Geophysics*, <https://doi.org/10.1002/2014RG000449>
4. Butler J., Montzka S., (2020) The NOAA Annual Greenhouse Gas Index, Earth System Research Lab. Global Monitoring Laboratory, <https://www.esrl.noaa.gov/gmd/aggi/aggi.html>
5. Wikipedia, Radiative forcing (2020)
6. Feinberg A, (2020) Urban Heat Island Amplification Estimates on Global Warming Using an Albedo Model, Vixra 2003.0088, DOI: 10.13140/RG.2.2.32758.14402/15 (recently accepted for publication, Journal of SN Applied Science (Oct. 2020))
7. IPCC, 2018: Global Warming of 1.5°C. An IPCC Special Report on the impacts of global warming of 1.5°C above pre-industrial levels and related global greenhouse gas emission pathways, in the context of strengthening the global response to the threat of climate change, sustainable development, and efforts to eradicate poverty [Masson-Delmotte, V., P. Zhai, H.-O. Pörtner, D. Roberts, J. Skea, P.R. Shukla, A. Pirani, W. Moufouma-Okia, C. Péan, R. Pidcock, S. Connors, J.B.R. Matthews, Y. Chen, X. Zhou, M.I. Gomis, E. Lonnoy, T. Maycock, M. Tignor, and T. Waterfield (eds.)].
8. Dunne D, (2018) Six ideas to limit global warming with solar geoengineering, CarbonBrief, <https://www.carbonbrief.org/explainer-six-ideas-to-limit-global-warming-with-solar-geoengin>

9. Pattyn F., Ritz C., Hanna E., Asay-Davis X., DeConto R., Durand G., Favier L., Fettweis X., Goelzer H., Gollledge N., Munneke P., Lenaerts J., Nowicki S, Payne A., Robinson A., Seroussi H., Trusel L., Broeke M., (2018) The Greenland and Antarctic ice sheets under 1.5 °C global warming, *Nature Climate Change*
10. Koen G. Helwegen1 , Claudia E. Wieners, A, Jason E. Frank L, and Henk A. Dijkstra, Complementing CO2 emission reduction by solar radiation management might strongly enhance future welfare, (2019) *Earth System Dynamics*
11. Latham, J., Rasch, P., Chen, C.-C., Kettles, L., Gadian, A., Gettelman, A., Morrison, H., Bower, K., and Choulaton, T.: Global temperature stabilization via controlled albedo enhancement of low-level maritime clouds, *Philos. T. R. Soc. A*, 366, 3969–3987, <https://doi.org/10.1098/rsta.2008.0137>, 2008.
12. Ahlm, L., Jones, A., Stjern C, Muri, H., Kravitz, B., and Kristjánsson, J. E.: Marine cloud brightening – as effective without clouds, *Atmos. Chem. Phys.*, 17, 13071, <https://doi.org/10.5194/acp-17-13071-2017>, 2017
13. Gabriel, C. J., Robock, A., Xia, L., Zambri, B., and Kravitz, B.: The G4 Foam Experiment: global climate impacts of regional ocean albedo modification, *Atmos. Chem. Phys.*, 17, 595–613, <https://doi.org/10.5194/acp-17-595-2017>, 2017
14. Seneviratne, S. I., Phipps, S. J., Pitman, A. J., Hirsch, A. L., Davin, E. L., Donat, M. G., Hirschi, M., Lenton, A., Wilhelm, M., and Kravitz, B.: Land radiative management as contributor to regional-scale climate adaptation and mitigation, *Nat. Geosci.*, 11, 88–96, <https://doi.org/10.1038/s41561-017-0057-5>, 2018.
15. Cho A, (2016) To fight global warming, Senate calls for a study of making Earth reflect more light, *Science*, <https://www.sciencemag.org/news/2016/04/fight-global-warming-senate-calls-study-making-earth-reflect-more-light>
16. Levinson, R., Akbari, H. (2010) Potential benefits of cool roofs on commercial buildings: conserving energy, saving money, and reducing the emission of greenhouse gases and air pollutants. *Energy Efficiency* 3, 53–109. <https://doi.org/10.1007/s12053-008-9038-2>
17. Paris Climate Accord, (2015) <https://unfccc.int/process-and-meetings/the-paris-agreement/what-is-the-paris-agreement>
18. Angel R., Feasibility of cooling the Earth with a cloud of small spacecraft near the inner Lagrange point (L1), (2006) PNAS.
19. Sánchez, Joan-Pau; McInnes, Colin R. (2015-08-26). "Optimal Sunshade Configurations for Space-Based Geoengineering near the Sun-Earth L1 Point". *PLoS ONE*. **10** (8): e0136648. doi:10.1371/journal.pone.0136648.
20. Zhao L., Lee X, Smith R., Oleson K. (2014) Strong, contributions of local background climate to urban heat islands, *Nature*. 10;511(7508):216-9. DOI: 10.1038/nature13462
21. Gunawardena K, Wells M, Kershawa T (2017) Utilising green and blue space to mitigate urban heat island intensity, *ScienceDirect*, doi: 10.1016, <https://www.sciencedirect.com/science/article/pii/S0048969717301754>
22. Dessler A., Zhang Z., Yang P., (2008) Water-vapor climate feedback inferred from climate fluctuations, 2003–2008, *Geophysical Research Letters*, <https://doi.org/10.1029/2008GL035333>
23. Manabe, S., and R. T. Wetherald (1967), Thermal equilibrium of the atmosphere with a given distribution of relative humidity, *J. Atmos. Sci.*, 24, 241–259
24. Cao C., Zhao J, Gong P, MA G., Bao D., Tian K., Wetland changes and droughts in southwestern China, *Geomatics, Natural Hazards and Risk*, Oct 2011,
25. Kimoto K. On the Confusion of Planck Feedback Parameters. *Energy & Environment*. 2009; 20(7):1057-1066. doi:10.1260/095830509789876835